

Giant microwave photo-conductance of a tunnel point contact with a bridged gate

A. D. Levin, G. M. Gusev, Z. D. Kvon, A. K. Bakarov, N. A. Savostianova, S. A. Mikhailov, E. E. Rodyakina, and A. V. Latyshev

Citation: [Applied Physics Letters](#) **107**, 072112 (2015); doi: 10.1063/1.4928733

View online: <http://dx.doi.org/10.1063/1.4928733>

View Table of Contents: <http://scitation.aip.org/content/aip/journal/apl/107/7?ver=pdfcov>

Published by the [AIP Publishing](#)

Articles you may be interested in

[Split-gate quantum point contacts with tunable channel length](#)

J. Appl. Phys. **113**, 024507 (2013); 10.1063/1.4774281

[Wide-band capacitance measurement on a semiconductor double quantum dot for studying tunneling dynamics](#)

Appl. Phys. Lett. **96**, 032104 (2010); 10.1063/1.3285180

[Radio-frequency point-contact electrometer](#)

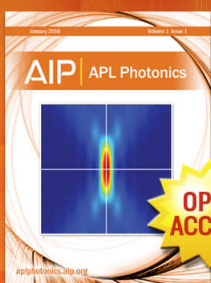
Appl. Phys. Lett. **88**, 203506 (2006); 10.1063/1.2205159

[Quantum point contact in a magnetic field: Far-infrared resonant heating observed in photoconductivity](#)

Appl. Phys. Lett. **75**, 3150 (1999); 10.1063/1.125260

[Parallel quantum-point-contacts as high-frequency-mixers](#)

Appl. Phys. Lett. **70**, 3251 (1997); 10.1063/1.119139



Launching in 2016!
The future of applied photonics research is here

AIP | APL
Photonics

Giant microwave photo-conductance of a tunnel point contact with a bridged gate

A. D. Levin,¹ G. M. Gusev,^{1,a)} Z. D. Kvon,^{2,3} A. K. Bakarov,^{2,3} N. A. Savostianova,⁴ S. A. Mikhailov,⁴ E. E. Rodyakina,^{2,3} and A. V. Latyshev^{2,3}

¹Instituto de Física da Universidade de São Paulo, 135960-170 São Paulo, SP, Brazil

²Institute of Semiconductor Physics, Novosibirsk 630090, Russia

³Novosibirsk State University, Novosibirsk 630090, Russia

⁴Institute of Physics, University of Augsburg, D-86135 Augsburg, Germany

(Received 11 May 2015; accepted 6 August 2015; published online 20 August 2015)

We study the microwave photo-response of a quantum point contact (QPC) formed on a GaAs/AlGaAs heterostructure with a high-electron-mobility two-dimensional electron gas. The QPCs are fabricated by two types of gates: a traditional split gate and a specially designed *bridged gate*. We observe a three orders of magnitude enhancement of the dark QPC conductance in the tunneling regime at the incident microwave power density of ~ 10 mW/cm². The response of the bridged-gate structure is more than ten times larger than that of the split-gate QPC. This giant effect and the difference between the two types of gates are explained by the influence of microwaves on the steady-state electron distribution function in the vicinity of the tunnel contact. Experimental results are in good quantitative agreement with theoretical calculations. The bridged-gate QPC can be used for the creation of highly sensitive detectors of electromagnetic radiation. © 2015 AIP Publishing LLC.

[<http://dx.doi.org/10.1063/1.4928733>]

A quantum point contact (QPC) is a narrow constriction between two wide conducting areas.¹ QPCs can be fabricated on a semiconductor structure with a two-dimensional electron gas (2DEG) by applying a negative bias to a split gate, see Figure 1(b). Dependent on the gate voltage, the resistance of such a split-gate QPC can be varied from $\simeq 10$ k Ω , when the conductance $\sigma = n\sigma_0$ is quantized^{2,3} in units of $\sigma_0 = 2e^2/h$ (n is integer), up to several M Ω in the tunneling regime.

It was shown⁴ that in the tunneling regime the split-gate QPC can be used for detection of microwave radiation (with the frequency $f < 40$ GHz in Ref. 4). In this letter, we experimentally study the microwave photo-response of a traditional (split gate) and a specially designed *bridged gate* QPC in the frequency range from 110 to 170 GHz. The bridged gate QPC consists of a single piece of a metal with a semi-elliptical narrowing, Fig. 1. We show that in the tunneling regime both QPCs, but especially the bridged gate one, become very sensitive to the irradiation: at the microwave power density ~ 10 mW/cm², we observe a two orders of magnitude (more than three orders of magnitude) exponential growth of the split-gate (bridged gate) QPC conductance. The physical mechanism of the detection is not restricted by the investigated frequencies. The bridged gate device can thus be used as an extremely sensitive detector of electromagnetic radiation in a broad frequency range.

Our samples are modulation doped GaAs/AlGaAs heterostructures with a 2DEG taken from two different wafers. The structure, referred to as A in this letter, has the density and the mobility of 2D electrons of about $(7 - 8) \times 10^{11}$ cm⁻² and 3×10^6 cm²/V s, respectively, which corresponds to the mean free path of $\simeq 60$ μ m, substantially exceeding the QPC

dimensions. The second structure B has the same density and a lower mobility 1.5×10^6 cm²/V s. The gate is fabricated on the surface of the heterostructure using electron beam lithography; the distance between the gate and the 2DEG is 90 nm. The samples are irradiated by microwaves with the frequency in the range from 110 to 170 GHz and the power density $\sim (1 - 10)$ mW/cm², corresponding to the microwave

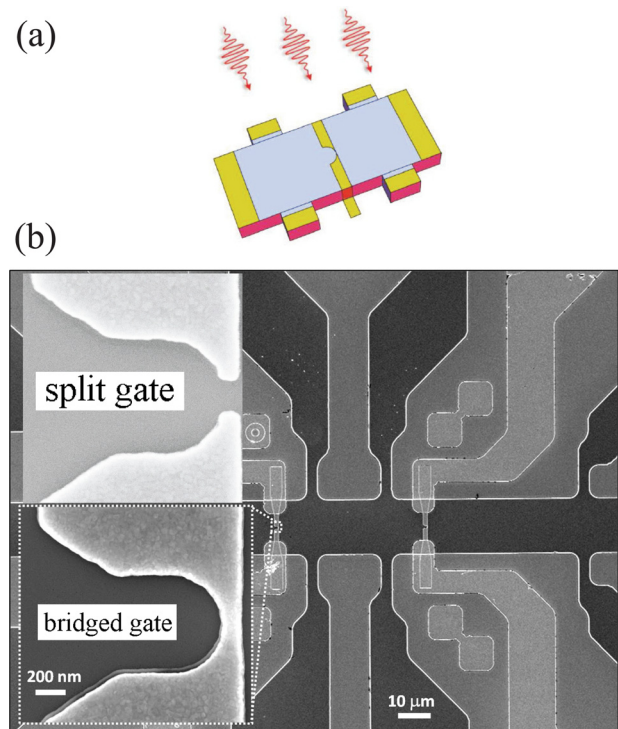


FIG. 1. (a) A schematic set-up of the bridged gate sample. (b) Top view of the sample. The magnified images of the split- and bridged-gates are shown in the left side of the figure.

^{a)}Electronic mail: gusev@if.usp.br

electric field of $E_{\omega} \sim (0.6 - 2)$ V/cm. The measurements were carried out in a VTI cryostat with a wave-guide delivering microwave radiation down to the sample and by using a conventional lock-in technique to measure the resistance $R = 1/\sigma$. The sample was rotated with respect to the orientation of the waveguide but no polarization dependence has been observed. Nine devices were studied and similar results have been obtained for all of them. Below, we focus on results obtained from two representative bridged gate devices.

Figure 2 illustrates the gate-voltage dependence of the conductance $\sigma(V_g)/\sigma_0$ at the frequency 149 GHz, temperature $T = 4.2$ K, and several microwave power attenuation factors for the bridged-gate sample from the wafer A. The results for the split-gate QPC are also shown for comparison. The conductivity exponentially decreases as the gate voltage becomes more negative, indicating a tunneling regime with the resistance up to several M Ω .

Microwaves strongly influence the conductance, especially in the tunneling regime, leading to a few orders of magnitude change of $\sigma(V_g)$. Such a strong effect cannot be explained by heating, since simultaneous measurements of

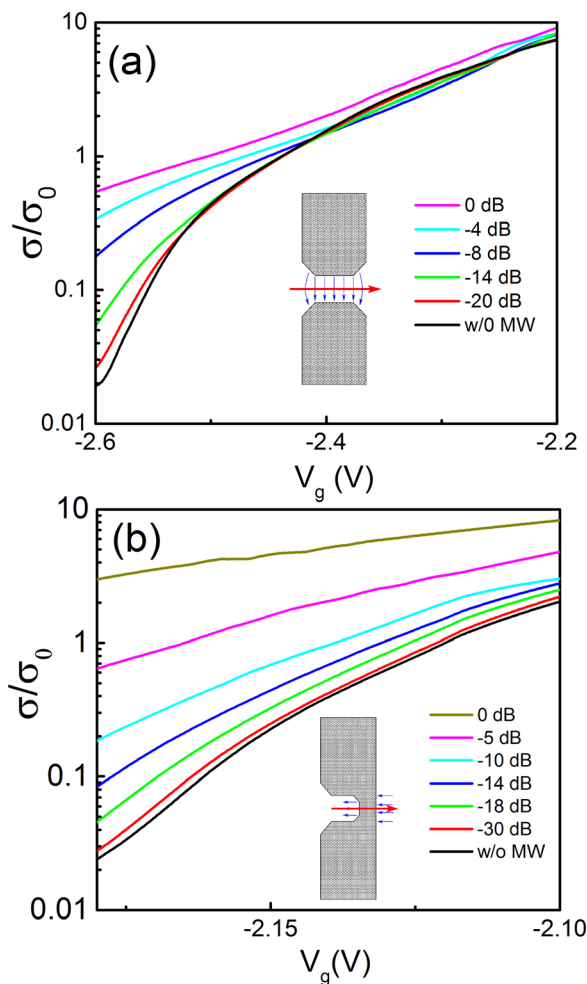


FIG. 2. The gate voltage dependence of the relative conductance $\sigma(V_g)/\sigma_0$ in (a) the split-gate and (b) the bridged-gate QPC devices (wafer A), at the microwave frequency 149 GHz, $T = 4.2$ K, and different values of the microwave power density. Insets schematically show the gate geometry and the direction of the electron tunneling (red horizontal arrows) and of the ac electric field in the tunnel barrier area (blue arrows).

the Shubnikov–de Haas oscillations in the Hall-bar part of the device (shown in the middle of Fig. 1) indicate a sample overheating by not more than 1 – 2 K, and the QPC conductance shows only a weak ($\sim 30\%$) growth when the temperature increases from 1.4 to 10 K. This excludes the bolometric mechanism of the photodetection in our devices. A similar behavior was observed in ballistic quantum dots.⁵

The bridged-gate devices are substantially more sensitive to the irradiation than the split-gate ones. This is illustrated in Figures 2 and 3 where results for the split- and bridged-gate samples from the wafer A are shown. In Figure 3, the gate voltages are chosen so that the dark conductances ($P = 0$) are approximately the same in both devices. The maximum power P_0 was also approximately the same both in the split- and bridged-gate QPCs which was independently controlled by the amplitude of the microwave induced resistance oscillations^{6–8} measured on the Hall bar. The split- and bridged-gate devices demonstrate more than one and three orders of magnitude growth of the conductance, respectively. Figures 4 and 5 show the gate voltage and power (P) dependencies of the conductance σ/σ_0 for one of the bridged-gate samples from the wafer B.

These experimental findings are explained as follows. Without the microwaves and at a large negative bias V_g , only a small amount of 2D electrons can tunnel through (or move over) the barrier, so that the dark current of the detector is very low. When the device is irradiated, the 2D electrons in the close vicinity of the QPC acquire an additional energy from the microwave field which increases their probability to get through or over the barrier. It is important to emphasize that the local ac electric field near the barrier can be *much larger* than the field of the incident wave, since the metallic areas covering the device (Figure 1) serve as antennas focusing the field in the QPC region. Moreover, the bridged gate has that advantage that the ac electric field is mainly polarized in the direction of the electron tunneling, thus substantially increasing the sensitivity of the QPC detector. Indeed, if an unpolarized radiation is incident on the thin metallic layer (gate) lying on top of the heterostructure, the field component parallel to the metallic edge is reduced, while the component perpendicular to it is increased, due to the

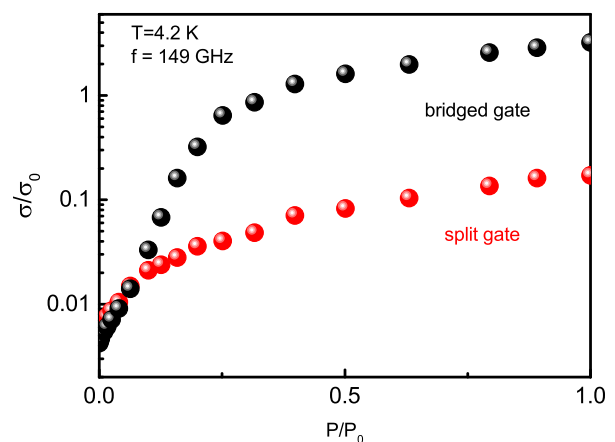


FIG. 3. The power dependencies of σ/σ_0 at the fixed gate voltage in the split-gate ($V_g = -2.65$ V) and bridged-gate ($V_g = -2.2$ V) QPC from the wafer A.

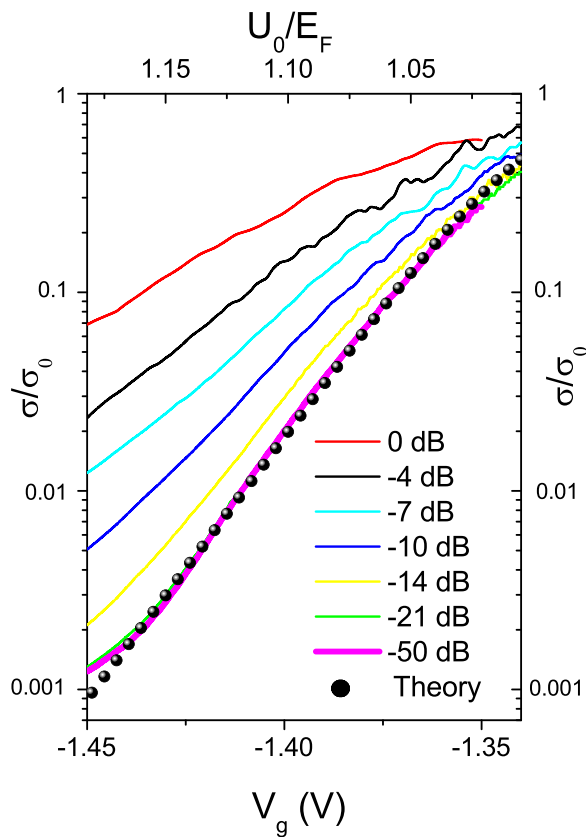


FIG. 4. The gate voltage dependence of σ/σ_0 of the bridged-gate QPC (wafer B) at the microwave frequency 145 GHz, $T = 4.2$ K, and different values of the microwave power density. The theory curve corresponds to Eq. (4) at $P = 0$ and $K_w/E_F = 0.006$.

screening of the electric field in the metal.⁹ In the split-gate structure, the local electric field is then mainly polarized perpendicular, while in the bridged-gate structure—parallel to the direction of the electron tunneling, see insets to Figure 2. This substantially increases the photocurrent in the latter case.

Quantitatively, the conductance of the tunnel barrier is described, in the Ohmic regime, by the formula

$$\frac{\sigma}{\sigma_0} = - \int_0^\infty dET(E) \frac{\partial F(E)}{\partial E}, \quad (1)$$

where E is the electron energy, $T(E)$ is the transmission coefficient of the tunnel barrier, and $F(E)$ is the electron distribution function near the QPC (in the absence of microwaves, $F(E)$ is given by the Fermi distribution). To estimate the transmission coefficient $T(E)$, we assume that the barrier has the form

$$U(x) = U_0 \cosh^{-2}(x/w), \quad (2)$$

where U_0 and w are the barrier height and width. Then, $T(E, U_0, K_w) = (1 + A^2)^{-1}$, where

$$A = \frac{\cosh\left(\pi\sqrt{U_0/K_w - 1/4}\right)}{\sinh\left(\pi\sqrt{E/K_w}\right)}, \quad (3)$$

and $K_w = \hbar^2/2mw^2$, Ref. 10. At low temperatures, the dark conductance is then $\sigma(V_g)/\sigma_0 \approx T(E_F)$ which is illustrated in Fig. 4 by the symbols labeled as “Theory.”

Microwaves modify the electron distribution function $F(E, P)$ in the vicinity of the barrier. To find the function $F(E, P)$, we solve the kinetic Boltzmann equation in the momentum-relaxation-time (τ) approximation at $\omega\tau \gg 1$. For the linearly polarized (in the x -direction) external electric field, we get the QPC conductance at $T = 0$

$$\frac{\sigma(P)}{\sigma_0} = \int_{-\pi}^{\pi} \frac{dx}{2\pi} \int_0^{2\pi} \frac{dy}{2\pi} [1 - 2\sqrt{P} \sin x \sin y] \times T\left(E_F [1 - 2\sqrt{P} \sin x \sin y]^2, U_0, K_w\right). \quad (4)$$

Here, $P = (eE_\omega/\omega p_F)^2$ is the dimensionless microwave-power parameter, and $p_F = \hbar k_F$ is the Fermi momentum. The calculations at $T \neq 0$ have been also done but the corresponding corrections have been found to be small.

The solid curves in Figure 5 show the calculated microwave power dependences $\sigma(P)/\sigma_0$ obtained from Eq. (4). All five curves have been fitted by the same values of the parameters $K_w/E_F = 0.006$ (corresponds to $k_F w = 12.9$) and $P_{max} = 0.0037$ (the maximum power level used in

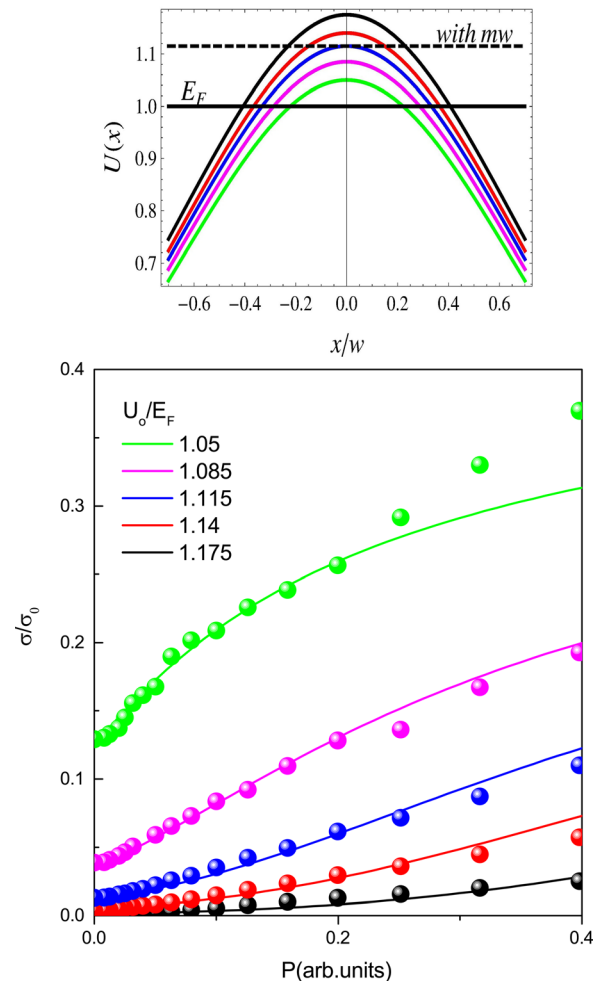


FIG. 5. The lower panel shows the power dependence of the conductance at fixed values of the gate voltage in the bridged-gate sample from the wafer B. The circles are experimental data, the lines are theoretical curves based on Eq. (4) with the fitting parameters $k_F w = 12.9$ and $P_{max} \approx 0.0037$. The top panel shows the potential energy of the barrier (2) at five values of U_0/E_F corresponding to the curves on the lower panel. The solid and dashed horizontal lines correspond to the effective Fermi energy without and with microwaves.

the experiment). The dimensionless barrier height U_0/E_F has then been found by fitting the theory to the experimental points at low P . Although the shape of the real potential barrier of the QPC is unknown and may substantially differ from the model expression (2), the agreement between the theory and experiment is surprisingly good in a very broad range of microwave powers.

The microwave power parameter $P_{max} = 0.0037$ extracted from the experiment corresponds to the maximum ac electric field $E_{\omega} = \omega p_F \sqrt{P_{max}}/e \simeq 70$ V/cm (calculated at $f = 145$ GHz and the density $n_s = 7 \times 10^{11}$ cm $^{-2}$). This value is about 35 times larger than the estimated electric field of the incident electromagnetic wave, which is a consequence of the focusing of the ac electric field by the gate antennas discussed above. In the split-gate devices, the same enhancement of the local ac field leads to a smaller photo-response since, in contrast to the bridged gate device, the ac electric field is mainly polarized perpendicular to the electron tunneling direction.

The proposed device can be used as a detector of microwave/terahertz/infrared radiation. Its responsivity can be estimated as follows. As seen from Fig. 3, the slope of the black-symbol curves at low P is about

$$\frac{d\sigma/\sigma_0}{dP/P_0} \simeq 0.05. \quad (5)$$

This can be rewritten as $dR/dP \simeq 0.05R^2/P_0R_0$, where $R_0 \simeq 1/\sigma_0 \simeq 12$ k Ω , $R \approx 1$ M Ω is the sample resistance, and P_0 is the incident power. Estimating the latter as the power density 10 mW/cm 2 times the squared length of the bridged gate ($\simeq 10 \times 10$ μ m 2 , see Fig. 1) and taking into account the current $\simeq 10^{-8}$ A in our sample, we get the responsivity of order of 10 6 V/W. This value is substantially higher than in other 2D electron gas detectors, see, e.g., Refs. 4, 11, and 12.

The large photoresponse in our experiment is achieved due to the strong enhancement of the local ac electric field near the sharp edges of the metallic gate placed on top of the heterostructure. These local fields can be *orders of magnitude larger* if the thickness of the metallic gate and the distance between the gate and the 2D layer (both ~ 100 nm in our experiment) will be smaller. For example, replacing the GaAs quantum well by a single atomic layer of semiconducting MoS $_2$, dielectric AlGaAs by few-layered hexagonal boron

nitride (h-BN), and the metallic gate by mono- or few-layered graphene would tremendously increase the local fields and, hence, the sensitivity of such a detector.

To conclude, we have observed a giant microwave photoresponse of the specially designed (bridged gate) QPC. Experimental observations are in very good agreement with the theory. The observed effect can be used for efficient detection of microwave, terahertz, and infrared radiation. A similar detector built using graphene related materials could have orders of magnitude higher sensitivity to the electromagnetic radiation.

The financial support of this work by RFBI (N 14-02-01246), RAS (programs 24 and 20), Grant No. SC-2968.2012.8, and FAPESP, CNPq (Brazilian agencies) is acknowledged. Also to perform this work, equipment from the ISP centre ‘‘Nanostructures’’ was used. N.S. and S.M. acknowledge financial support by the European Union under the FET-open grant GOSFEL and the program Graphene Flagship (No. CNECT-ICT-604391).

- ¹H. van Houten and C. W. J. Beenakker, *Phys. Today* **49**(7), 22 (1996).
- ²B. J. van Wees, H. van Houten, C. W. J. Beenakker, J. G. Williamson, L. P. Kouwenhoven, D. van der Marel, and C. T. Foxon, *Phys. Rev. Lett.* **60**, 848 (1988).
- ³D. Wharam, T. J. Thornton, R. Newbury, M. Pepper, H. Ahmed, J. E. F. Frost, D. G. Hasko, D. C. Peacock, D. A. Ritchie, and G. A. C. Jones, *J. Phys. C: Solid State Phys.* **21**, L209 (1988).
- ⁴P. S. Dorozhkin, S. V. Tovstonog, S. A. Mikhailov, I. V. Kukushkin, J. H. Smet, and K. von Klitzing, *Appl. Phys. Lett.* **87**, 092107 (2005).
- ⁵Z. D. Kvon, G. M. Gusev, A. D. Levin, D. A. Kozlov, E. E. Rodyakina, and A. V. Latyshev, *Pis'ma Zh. Eksp. Teor. Fiz.* **98**, 806 (2013), http://www.jetpletters.ac.ru/ps/2027/article_30564.shtml; *JETP Lett.* **98**, 713 (2014).
- ⁶M. A. Zudov, R. R. Du, J. A. Simmons, and J. L. Reno, *Phys. Rev. B* **64**, 201311 (2001).
- ⁷R. G. Mani, J. H. Smet, K. von Klitzing, V. Narayanamurti, W. B. Johnson, and V. Umansky, *Nature* **420**, 646 (2002).
- ⁸M. A. Zudov, R. R. Du, L. N. Pfeiffer, and K. W. West, *Phys. Rev. Lett.* **90**, 046807 (2003).
- ⁹S. A. Mikhailov and N. A. Savostianova, *Phys. Rev. B* **74**, 045325 (2006).
- ¹⁰L. D. Landau and E. M. Lifshitz, *Quantum Mechanics (Non-Relativistic Theory)* (Elsevier, Oxford, 1994).
- ¹¹M. I. Dyakonov and M. Shur, *IEEE Trans. Electron Devices* **43**, 380 (1996).
- ¹²J.-Q. Lü, M. S. Shur, J. L. Helser, L. Sun, and R. Weikle, *IEEE Electron Device Lett.* **19**, 373 (1998).